

X-ray Constraints on the Ly α Escape Fraction

Zhen-Ya Zheng^{1,2}; Sangeeta Malhotra²; Jun-Xian Wang¹; James E. Rhoads²; Steven L. Finkelstein³; Eric Gawiser⁴; Caryl Gronwall⁵; Lucia Guaita⁶; Kim K. Nilsson⁷; Robin Ciardullo⁵

ABSTRACT

We have coadded X-ray flux of all known Ly α emitters in the 4 Msec Chandra Deep Field South (CDF-S) region, to place sensitive upper limits on the average unobscured star-formation rate (SFR $_X$) in these galaxies. A very small fraction of Ly α galaxies in the field are individually detected in the X-rays, implying a low fraction of AGN activity. After excluding the few X-ray detected Lyman alpha emitters (LAEs), we stack the undetected LAEs located in the 4 Ms CDF-S data and 250 ks Extended CDF-S (ECDFS) data, and compute a $1-\sigma$ upper limit on SFR $_X < 14, 28, 28, 140, 440, 880$ M $_{\odot}$ yr $^{-1}$ for LAEs located at $z = 2.1, 3.1, 3.2, 4.5, 5.7$ and 6.5 , respectively. The upper limit of SFR $_X$ in LAEs can be then be compared to SFR $_{Ly\alpha}$ derived from Ly α line and thus can constrain on the Ly α escape fraction ($f_{Ly\alpha}^{Esc}$). We derive a lower limit on $f_{Ly\alpha}^{Esc} > 14\%$ (84 % confidence level, 1σ lower limit) for LAEs at redshift $z \sim 2.1$ and $z \sim 3.1-3.2$. At $z > 4$, the current LAE samples are not of sufficient size to constrain SFR $_X$ well. By averaging all the LAEs at $z > 2$, the X-ray non-detection constrains $f_{Ly\alpha}^{Esc} > 17\%$ (84 % confidence level, 1σ lower limit), and rejects $f_{Ly\alpha}^{Esc} < 5.7\%$ at the 99.87% confidence level from $2.1 < z < 6.5$.

Subject headings: galaxies: active — galaxies: high-redshift — galaxies: starburst — X-rays: galaxies

1. INTRODUCTION

Ly α emission, the 1216 Å ($n = 2 \rightarrow 1$) transition of hydrogen in emission, is a prominent tracer of ionizing photons produced by young stars. This line can carry up to $\sim 6\%$ of the bolometric

¹Department of Astronomy, University of Science and Technology of China, Hefei, Anhui 230026, China; zhengzy@mail.ustc.edu.cn

²School of Earth and Space Exploration, Arizona State University, Tempe, AZ 85287

³George P. and Cynthia Woods Mitchell Institute for Fundamental Physics and Astronomy, Department of Physics and Astronomy, Texas A&M University, College Station, TX 77843

⁴Department of Physics and Astronomy, Rutgers University, 136 Frelinghuysen Rd., Piscataway, NJ 08854

⁵Department of Astronomy & Astrophysics, Penn State University, State College, PA 16802

⁶Department of Astronomy, Oscar Klein Center, Stockholm University, AlbaNova, Stockholm SE-10691, Sweden

⁷European Southern Observatory, Karl-Schwarzschild-StraBe 2, 85748 Garching bei Munchen, Germany

luminosity of a star forming galaxy (Partridge & Peebles 1967), therefore it is an easy handle for detection of both star forming galaxies and active galactic nuclei (AGN, where Ly α emission is turned from the ionizing photons produced at the accretion disk around the central massive black hole) at redshifts $z > 2$. The Ly α line-search technique has been used successfully to identify samples of high redshift galaxies for over a decade, using narrowband images (e.g., Cowie & Hu 1998; Rhoads et al. 2000, 2003; Malhotra & Rhoads 2002, Gawiser et al. 2007; Finkelstein et al. 2008, 2009; Guaita et al. 2010) and spectroscopic surveys (e.g., Pirzkal et al. 2004, Deharveng et al. 2008, Martin et al. 2008, Rhoads et al. 2009, and Blanc et al. 2010). There are thousands of photometrically selected Ly α emitters, with hundreds of spectroscopic confirmations (e.g., Hu et al. 2004, Dawson et al. 2007, Wang et al. 2009) at redshifts ranging from $z \approx 0.3$ (Deharveng et al. 2008) to $z \approx 7$ (Iye et al. 2006).

However, interpreting the Ly α line is not trivial, because Ly α photons are resonantly scattered when they interact with the surrounding neutral hydrogen in the inter-stellar medium (ISM). These radiative transfer effects can be quite complex when considering the presence of dust in multiphase media (Neufeld 1991, Hansen & Oh 2006; Finkelstein et al. 2009c). The resonant nature of the Ly α line can be measured through the escaping fraction of Ly α photons ($f_{Ly\alpha}^{Esc}$), defined as the observed Ly α line flux to the intrinsic Ly α line flux ratio. Various methods have been applied to estimate the intrinsic Ly α emission. For example, under the case B recombination theory, intrinsic Ly α line flux can be converted from the H α line flux corrected by dust extinction E(B-V) (e.g., Atek et al. 2009 for $z \sim 0.3$ LAEs, Hayes et al. 2010 for $z \sim 2.25$ LAEs, and Finkelstein et al. 2011 for $z \sim 2.3$ - 2.5 LAEs). Since Ly α photons trace of young stars, the intrinsic Ly α emission is connected to the intrinsic star formation rate (SFR).

X-ray observations of high-redshift star-forming galaxies can be used as an indirect tracer of the SFR, since supernovae (SNe), hot interstellar gas (i.e., $T > 10^{6-7}$ K), and high-mass X-ray binaries (HMXBs) are all products of very massive young stars. Low-mass X-ray binaries also contribute to X-ray emission from galaxies, but they have longer evolutionary time scales (on the order of the Hubble time), and therefore track the integrated star-formation history of galaxies (i.e., the total stellar mass). This trend is well shown for nearby galaxies, as the relationship of galaxy stellar mass and SFR from X-ray observations from Colbert et al. (2004):

$$L_{2-8keV} = \alpha \times M_* + \beta \times SFR_X, \quad (1)$$

here L_X , M_* , and SFR_X have units of ergs s^{-1} , M_\odot , and $M_\odot \text{ yr}^{-1}$, respectively, and constants $\alpha = 1.3 \times 10^{29} \text{ ergs s}^{-1} M_\odot^{-1}$ and $\beta = 0.7 \times 10^{39} \text{ ergs s}^{-1} (M_\odot \text{ yr}^{-1})^{-1}$. Gilfanov, Grimm & Sunyaev (2004) compare the local galaxy sample with Hubble Deep Field North galaxies and suggest a cut-off luminosity $\sim 5 \times 10^{40} \text{ erg s}^{-1}$ for HMXBs, above which the SFR_X and L_X has a linear relationship for star-forming galaxies. Other studies, Nandra et al. 2002, Grimm et al. 2003, Ranalli et al. 2003, Persic et al. 2004, also show that non-nuclear X-ray emission from galaxies can be used as a star formation rate indicator for high redshift star-forming galaxies, which might be dominated by

HMXBs. These relations are all consistent with Ranalli et al. (2003), as

$$\begin{aligned} SFR_X &= 2.2 \times 10^{-40} L_{0.5-2} \text{ M}_\odot \text{ yr}^{-1}, \\ SFR_X &= 2.0 \times 10^{-40} L_{2-10} \text{ M}_\odot \text{ yr}^{-1}, \end{aligned} \quad (2)$$

, and all the relations are calibrated with the total SFR from far-infrared (FIR) and ultraviolet (UV) bands for local and high- z ($z \sim 1$) star-forming galaxies (in the Chandra Deep Field North and South, CDF-N and CDF-S, where the deepest X-ray observations exist). These relationships thus allow one to derive the intrinsic (dust-free) SFR from star-forming galaxies directly from X-ray observations.

The SFR_X of high redshift star-forming galaxies was measured by Nandra et al. (2002), who detected a stacked X-ray signal of $z \approx 3$ Lyman Break Galaxies (LBGs) in the Hubble Deep Field North. The average X-ray luminosity of $z \approx 3$ LBGs is $L_{2-10} = 3.4 \times 10^{41} \text{ ergs s}^{-1}$ (6σ significance), implying a $SFR_X = 64 \pm 13 \text{ M}_\odot \text{ yr}^{-1}$, in excellent agreement with the extinction-corrected UV estimates. In the same field, Laird et al. (2006) found the average SFR_X of $42.4 \pm 7.8 \text{ M}_\odot \text{ yr}^{-1}$ for $z \sim 3$ LBGs. Additionally, Lehmer et al. (2005) reported the average SFR_X of $\sim 30 \text{ M}_\odot \text{ yr}^{-1}$ for $z \sim 3$ LBGs in CDF-S (old 1 Ms *Chandra* exposure). Lehmer et al. also stacked LBGs in CDF-S at $z \sim 4, 5, \text{ and } 6$, and did not obtain significant detections ($< 3 \sigma$), deriving rest-frame 2.0-8.0 keV luminosity upper limits (3σ) of 0.9, 2.8, and $7.1 \times 10^{41} \text{ ergs s}^{-1}$, corresponding to SFR_X upper limits of 18, 56 and $142 \text{ M}_\odot \text{ yr}^{-1}$, respectively. Note also that a $\sim 3 \sigma$ stacking signal of the optically bright subset (brightest 25%) of LBGs at $z \sim 4$ was detected, corresponding to an average SFR_X of $\sim 28 \text{ M}_\odot \text{ yr}^{-1}$. These studies demonstrate the value of stacking the deepest X-ray observations to measure star formation activity, with little sensitivity to dust.

Since LAEs are thought to be less massive and much younger than LBGs at high-redshift (e.g., Venemans et al 2005; Pirzkal et al 2007; Finkelstein et al 2008, 2009c), and the AGN fraction in LAEs is also very small ($< 5\%$, e.g., Zheng et al. 2010), the LAEs' X-ray emission is probably due to the newly formed HMXBs. An X-ray detection could give us a more accurate unbiased SFR estimate, or more properly an upper limit, since faint AGN may contribute to the X-ray flux. The first X-ray observations of high-redshift LAEs were presented in Malhotra et al. (2003) and Wang et al. (2004) at $z \sim 4.5$ with two 170 ks *Chandra* exposures. No individual LAEs were detected, and a 3σ upper limit on the X-ray luminosity ($L_{2-8\text{keV}} < 2.8 \times 10^{42} \text{ ergs s}^{-1}$) was derived by an X-ray stacking method (Wang et al. 2004). From a stacking analysis of the non-detected LAEs in the much deeper 2 Ms CDF-S field and a larger 250 ks ECDFS field, Guaita et al. (2010), Gronwall et al. (2007) and Zheng et al. (2010) found a smaller 3σ upper limit on the luminosity of $\sim 1.9 \times 10^{41} \text{ ergs s}^{-1}$, $3.1 \times 10^{41} \text{ ergs s}^{-1}$, $2.4 \times 10^{42} \text{ ergs s}^{-1}$ at $z = 2.1$, $z = 3.1$ and $z = 4.5$, respectively. These imply upper limits of unobscured average $SFR_X < 43, 70 \text{ and } 290 \text{ M}_\odot \text{ yr}^{-1}$, respectively (using the L_X - SFR calibration of Ranalli et al. 2003). The previous results are not surprising, since we would expect that LAEs have lower SFR rates than LBGs.

With the intrinsic SFR from X-ray and the observed SFR from the observed Ly α photons, we can measure the Ly α escape fraction of $f_{Ly\alpha}^{Esc}$ as the ratio of $SFR_{Ly\alpha}$ and SFR_X , here $SFR_{Ly\alpha}$ is

converted under Kennicutt (1998) with Case B recombination assumption. The $f_{Ly\alpha}^{Esc}$ is important at high- z , since the Ly α emission is apparent in a large fraction of high- z galaxies, and becomes the only spectral feature we have access to. Statistical analysis of $f_{Ly\alpha}^{Esc}$, especially its evolution with redshift, can therefore provide us with independent estimates of how various properties of the galaxy evolve over cosmic time. The $f_{Ly\alpha}^{Esc}$ has been investigated for Ly α emitters at different redshifts with intrinsic SFR from UV or H α photons, from $z \approx 0.3$ to $z \approx 4$. At $z \approx 0.3$, Atek et al. (2009) showed that $f_{Ly\alpha/H\alpha}^{Esc}$ ¹ spans a wide range and decreases with increasing dust extinction. At $z \approx 2.25$, Hayes et al. (2010) estimated an average escape fraction of $f_{Ly\alpha/H\alpha}^{Esc} \sim 5\%$ with a double blind survey targeting Ly α and H α at $z = 2.25$. At $z \approx 1.9$ – 3.8 , Blanc et al. (2010) got a median $f_{Ly\alpha/UV-corr}^{Esc}$ of 22% from 98 LAEs detected through integral-field spectroscopy surveys. In simulation, Nagamine et al. (2010) predicted $f_{Ly\alpha}^{Esc} \simeq 0.1$ (0.15) for LAEs at $z = 3$ (6) through cosmological smoothed-particle hydrodynamics (SPH) simulations.

In this paper, we present an independent analysis of the Ly α escape fraction at $2 < z < 6.5$, using X-ray emission as a tracer of the intrinsic SFR. We use the new 4 Msec *Chandra* X-ray image in the CDF-S, which include LAEs at $z=0.3$ selected by GALEX, and narrowband selected LAEs at $z = 2.1, 3.1, 3.15, 4.5, 5.7, \text{ and } 6.5$. By comparing the ratio of derived SFRs from observed Ly α line flux and X-ray, we will perform an independent check on the evolution of the Ly α escape fraction for LAEs from an X-ray view. The optical samples and X-ray data are presented in §2, and the X-ray detection and stacking results on LAEs are presented in §3. The results and discussion on X-ray constrained Ly α escape fraction are presented in §4 and §5, respectively.

2. OPTICAL AND X-RAY DATA

In the *Chandra* Deep Field South region, samples of Ly α emitters have been observed at various redshifts, including Ly α emitters at $z = 0.3$ (Deharveng et al. 2008), $z = 2.1$ (Guaita et al. 2010), $z = 3.1$ (Gronwall et al. 2007, Ciardullo et al. 2011 in prep.), $z = 3.15$ (Nilsson et al. 2007), $z = 4.5$ (Finkelstein et al. 2009), $z = 5.7$ (Wang et al 2005) and $z = 6.5$ (Rhoads in prep.). The LAEs at $z = 0.3$ were selected by the Ly α emission line in the GALEX spectra. At higher redshift ($z > 2$), all the samples were selected through ground-based narrowband selection, which typically have a spectroscopic confirmation fraction greater than 70% (Dawson et al. 2007, Gawiser et al. 2007, Wang et al. 2009). In this paper we focus on LAEs covered in the CDF-S proper region. The number of LAEs at each redshift and their stacked X-ray properties are presented in Tables 1 and 2.

The 4 Ms *Chandra* Advanced CCD Imaging Spectrometer (ACIS) exposure of the CDF-S is

¹Here H α in the subscript means that the Ly α escape fraction is estimated with intrinsic SFR from H α emission. Since there are more than one way to get the intrinsic SFR (e.g., from UV-corrected luminosity in Blanc et al. 2010 and X-ray luminosity in this work), we will use different subscripts to separate the Ly α escape fraction estimated from different intrinsic SFR.

composed of 52 individual ACIS-I observations, 9 of which were obtained in 2000, 12 from September to November 2007, and 31 from March to July 2010. The event-2 file and exposure-map files are available at the *Chandra* website (<http://cxc.harvard.edu/cdo/cdfs.html>). To search for potential X-ray counterparts for our LAEs, we run the CIAO software WAVDETECT on the X-ray images in three bands (0.5 – 2 keV, 2 – 7 keV and 0.5 – 7 keV band). With a detection threshold of 1×10^{-6} , we detect 642 sources. Luo et al. (2008) published the X-ray source catalogs of the original 2-Ms CDF-S data with the same detection threshold. By combining the two we get 712 X-ray sources. We use this catalog of 712 X-ray sources for the following source cross-match and source-masking processes.

3. X-RAY IMAGING RESULTS

3.1. Individual detections in Chandra images.

We search for X-ray counterparts for individual LAEs within a $2''$ radius. At $z \sim 0.3$, one of two LAEs located in the CDF-S region was detected in the 2 Msec X-ray catalog (Luo et al. 2008), and the other one (53.2803, -27.7424) was newly detected with 4 Msec *Chandra* data. Their UV and X-ray properties are presented in Table 1. These galaxies have spectral signatures of star-forming galaxies (Cowie et al. 2010), consistent with their low X-ray luminosities.

X-ray counterparts have previously been detected for a small fraction ($< 5\%$) of the LAEs at higher redshifts. Guaita et al. (2010) detected X-rays from 10 of their 216 $z = 2.1$ LAEs in the ECDF-S region, using the 2Msec *Chandra* image for those LAEs in the central CDF-S (Luo et al. 2008), and the 250 ksec *Chandra* image (Lehmer et al. 2005) for those in the wider ECDFS. Gronwall et al. (2007) and Ciardullo et al (in prep.) selected 278 LAE candidates at $z = 3.1$, and only 5 were X-ray detected. At $z = 4.5$, only 1 of 113 LAE candidates show X-ray detection in ECDF-S field (Zheng et al. 2010) and is classified as an AGN at the same redshift, and no X-ray detections were found for 24 LAE candidates at $z = 3.15$ (Nilsson et al. 2007), 25 LAE candidates at $z = 5.7$ (Wang et al. 2005), or 11 LAE candidates at $z = 6.5$ (Rhoads et al. in prep.). In this paper, these previous X-ray detections are excluded, and we find no new X-ray detection with 4 Ms *Chandra* exposure.

We calculate the X-ray signal-to-noise ratio for the X-ray non-detected LAEs, all of which show $S/N < 3$. The S/N ratios were calculated as $S/N = S/(\sqrt{T + 0.75} + 1)$ (Gehrels 1986), where S and T are the net counts and total counts extracted from their 50% *Chandra* ACIS PSF circles² in 0.5-2, 2-7 and 0.5-7 keV band respectively. To convert from X-ray counts to fluxes, we have assumed a powerlaw spectrum with photon index of $\Gamma = 2$ (except where explicitly stated otherwise), which generally represents the X-ray spectra of both starburst galaxies (e.g., Lehmer et al. 2008) and

² The background counts ($B = T - S$) were estimated from an annulus with $1.2R_{95\%PSF} < R < 2.4R_{95\%PSF}$ (after masking out nearby X-ray sources).

type 1 AGNs. When converted from PSF-corrected count-rate to flux, the full and hard bands were extrapolated to the standard upper limit of 10 keV. All X-ray fluxes and luminosities presented in this paper have been corrected for Galactic absorption (Dickey & Lockman 1990). The 4 Ms CDF-S data reaches on-axis sensitivity limits of X-ray luminosity $L_{g10}(L_{2-10}) \approx [41.7, 42.1, 42.1, 42.5, 42.7, 42.8]$ at $z = [2.1, 3.1, 3.2, 4.5, 5.7, 6.5]$.

3.2. Stacking analysis

We stacked the X-ray data at the positions of the non-detections at each redshift, following Zheng et al. (2010). After masking out the X-ray detected sources with 95% PSF circles, we co-added the net and background counts of the X-ray non-detected LAEs in each sample. The stacked net and background counts in the soft, hard and 0.5-7 keV band, as well as the summed effective Chandra exposure time are presented in Tab. 2. We used the 95% PSF region for bright source extraction, and 50% PSF region for upper limit estimate ³. The results are about 0.2 dex lower than upper limit from 95% PSF extraction.

In Figure 1 we plot the 1σ upper limits (upper plot) on the mean X-ray luminosity for each studied redshift in the selection region (parameterized by the maximum off-axis angle θ for inclusion in the sample), and the S/N ratios of the stacked signals are also plotted in the lower part. From Figure 1 we can see that the mean luminosity can be better constrained by excluding LAEs with larger off-axis angles. This is mainly because the Chandra ACIS has much larger PSF and much lower collection area at larger off-axis angles, so that including those LAEs with large off-axis angles would bring strong fluctuations to the signal without necessarily increasing the S/N. In the following study, we exclude those LAEs with ACIS off-axis angle above $6'$, and the number of LAEs used for stacking and their stacked results at relative redshifts are presented in Table 2.

4. Results: $f_{esc}^{Ly\alpha}$ from X-rays

The average $f_{Ly\alpha}^{Esc}$ calculated using $SFR_{Ly\alpha}$ and SFR_X for LAEs at different redshifts are presented in Table 3. Here $SFR_{Ly\alpha}$ is star-formation rate estimated from the photometric Ly α line emission and assuming Case-B conditions (Kennicutt 1998: $SFR_{Ly\alpha} = 9.1 \times 10^{-43} \times L_{Ly\alpha}$). SFR_X is the unobscured SFR (dust-free SFR), calculated using Ranalli et al.'s calibration (equation 2). We only take the soft band upper limits for $z > 2$ LAEs, because soft band flux are more sensitive than the total band and hard band, and at $z > 2$, the observed soft band X-ray photons are closer to rest-frame hard photons, and therefore more robust to a change in photon index Γ (see Figure 2 of Wang et al. 2007).

³Polynomial approximation of the off-axis ACIS-I PSF, see <http://cxc.harvard.edu/chandra-users/0192.html>.

At $z \sim 0.3$, we have both $L_{0.5-2keV}$ and $L_{2-10keV}$ for the two LAEs, so the SFR_X can be estimated with Colbert et al. (2004) or Ranalli et al. (2003). Using the relation from Colbert et al. (equation 1) and the stellar mass from Finkelstein et al. (2009a), which was derived via spectral energy distribution fitting, we find $SFR_X \sim 100-500 M_\odot \text{ yr}^{-1}$. The Ly α -derived SFR is much lower, at $0.3 - 2 M_\odot \text{ yr}^{-1}$, implying a large amount of dust extinction and $f_{Ly\alpha/X}^{Esc} \sim 0.3-0.4\%$. With the relation from Ranalli et al. (equation 2), we can get $SFR_X = 16-80 M_\odot \text{ yr}^{-1}$ or $3.5-14 M_\odot \text{ yr}^{-1}$ from SFR_X-L_{2-10} or $SFR_X-L_{0.5-2}$, implying the Ly α escape fraction of 2-3% and 9-14%, respectively. Finkelstein et al. (2009b) also derived the dust extinction of $A_{1200} = 0.9\sim 2$ from the SED fitting, corresponding to $f_{Ly\alpha/UV-corr}^{Esc} = SFR_{Ly\alpha}/(SFR_{UV}/10^{-A_{1200}/2.5}) = 2-5\%$ (see table 3), which favors $SFR_X - L_{2-10}$ relation of Ranalli et al. as $f_{Ly\alpha/X}^{Esc} = SFR_{Ly\alpha}/SFR_X \sim 2-3\%$. However, we cannot exclude the possibility that the X-ray flux is contaminated by emission from a buried central massive black holes, even through these objects have been spectroscopically confirmed as star forming galaxies by Cowie et al. 2010, since LAEs at $z \sim 0.3$ show a much higher AGN fraction than at $z > 2$ of $\sim 15\%-40\%$ (Scarлата et al. 2009; Cowie et al. 2010; Finkelstein et al. 2009), greatly exceeding the AGN fraction at $z > 2$. These two galaxies are located at the edge of ACIS-I with the 95% PSF radius of $8''-10''$, so we cannot resolve the X-ray radiation from the central massive black holes. The moderate X-ray obscuration of $NH \sim 2-3 \times 10^{22} \text{ cm}^{-2}$ derived, supports the hypothesis that X-rays arise in a buried central black hole. So the $f_{Ly\alpha}^{Esc}$ at $z \sim 0.3$ from $SFR_X - L_{2-10}$ relation of Ranalli et al. should be lower limits, here we get $f_{Ly\alpha}^{Esc} \sim 2-9\%$ and 3-14% for these two $z \sim 0.3$ LAEs, respectively.

At $z > 2$, we do not obtain an X-ray detection after stacking the 69 star-formation dominated LAEs in the central CDF-S field, or after stacking the 351 LAEs in the ECDFS field (see Table 2). With the relationship of $L_{2-10keV}$ (from soft band flux at the observed frame) and SFR_X from Ranalli et al. (2003), we get the upper limits on the intrinsic (dust-free) SFR as $SFR_X < [14, 28, 28, 139, 440, 876] M_\odot \text{ yr}^{-1}$ for LAEs at $z = [2.1, 3.1, 3.2, 4.5, 5.7, 6.5]$. The observed SFRs from the Ly α line are about 1.9, 2.6 and 2.3 $M_\odot \text{ yr}^{-1}$ for $z = 2.1, 3.1$ and 3.2 LAEs on average, and $\sim 5 M_\odot \text{ yr}^{-1}$ for $z > 4$ LAEs. The ratio $SFR_{Ly\alpha} / SFR_X$ measures the Ly α escape fraction: $f_{Ly\alpha/X}^{Esc} = SFR_{Ly\alpha} / SFR_X$ (see Table 3). This is plotted in figure 2, showing the constraints on $f_{Ly\alpha}^{Esc}$ as a function of redshift. At $z = 2.1$, the Ly α escape fraction of LAEs is above 14%. At $z = 3.1$ and 3.2, the $f_{esc}^{Ly\alpha}$ is greater than 8% and 9%, separately. Combining the two samples at $z \sim 3$, we increase the upper limit to $f_{esc}^{Ly\alpha} > 14\%$, the same as the upper limit at $z = 2.1$. At higher redshift, the limits are weaker due to a larger luminosity distance, and comparatively smaller Ly α sample sizes.

If the Ly α emitters don't evolve from $z = 3.2$ to $z = 2.1$, then we can combine the samples in this redshift range to obtain a more robust limit on the escape fraction. A $1-\sigma$ upper limit on soft band flux is derived as $f_{0.5-2keV} < 8.5 \times 10^{-19} \text{ ergs cm}^{-2} \text{ s}^{-1}$. This implies an $SFR_{Ly\alpha}/SFR_X > 14\% \sim 28\%$ (due to the different $SFR_{Ly\alpha}$ average value) during the redshift range $2.1 \leq z \leq 3.2$. This value is consistent with the median value of $f_{Ly\alpha/UV-corr}^{Esc} \sim 22\%$ from blank fields IFU spectroscopically-selected LAEs at $1.9 < z < 3.8$ (Blanc et al. 2010), but larger than the value of $f_{Ly\alpha/H\alpha}^{Esc} \sim 5\%$ of Hayes et al. (2010) from H α to Ly α luminosity functions of all H α detected

objects at $z = 2.2$. Note that our fraction is for particular Ly α emitting galaxies, while Hayes' fraction is essentially a volume average that includes galaxies we'd never select as Ly α emitters.

5. Discussion

5.1. $f_{Ly\alpha}^{Esc}$ with 4 Msec CDF-S data

There is no X-ray detection for Ly α emitters coadded at any individual redshift bin ($z > 2$). By coadding the 53 Ly α emitters at $2.1 \leq z \leq 3.2$, we reach an X-ray flux limit of 8.5×10^{-19} ergs $\text{cm}^{-2} \text{s}^{-1}$ (1σ), but still do not detect X-ray photons from these galaxies. This means that the star-formation rate is truly low, as indicated by the Ly α line strength. To increase our sensitivity to detect the star formation rate of LAEs, which is relatively low when compared to continuum-selected star-forming galaxies at comparable redshifts, we coadd all the undetected Ly α emitters between redshifts 2 and 6.5. The average x-ray emission is still undetected at a 1-sigma flux level of 7.6×10^{-19} ergs $\text{cm}^{-2} \text{s}^{-1}$. To convert the flux into luminosity and hence SFR, we need to model the redshift distribution of the sources.

Let us, instead, predict the expected X-ray counts on this average image of Ly α galaxies. Assuming the Ly α escape fraction for LAEs is $f_{Ly\alpha}^{Esc}$, then $\text{SFR}_X = \text{SFR}_{Ly\alpha} / (f_{Ly\alpha}^{Esc}) = 2.0 \times 10^{-40} L_X$, we get

$$L_{2-10keV, \text{ rest}} = \frac{\text{SFR}_{Ly\alpha}}{2.0 \times f_{Ly\alpha}^{Esc}} \times 10^{40} \text{ ergs s}^{-1}. \quad (3)$$

If we assume that all LAEs have an effective X-ray photon index of $\Gamma = 2$, then with the X-ray count-rate to flux conversion of 6.64×10^{-12} erg/ cm^2 at soft band and $\text{SFR}_{Ly\alpha}$ from the table 3, we estimate that the average X-ray photons at ~ 4 Ms CDF-S for LAEs should be $(\frac{\text{SFR}_{Ly\alpha}}{f_{Ly\alpha}^{Esc} \times 100} \times [8.0, 3.0, 3.0, 1.3, 0.7, 0.5])$ for LAEs at $z = [2.1, 3.1, 3.2, 4.5, 5.7, 6.5]$. This means that we should observe ~ 3 soft X-ray photons per $z = 2.1$ LAE galaxy in the 4 Ms CDF-S field when $f_{Ly\alpha}^{Esc} \sim 5\%$, and the observed expected soft X-ray photons decrease to ~ 1 when $f_{esc}^{Ly\alpha}$ increases to 15% . Since the background X-ray photons per point source on the ACIS-I CCDs varies from position to position, we take the background value extracted from each LAE candidate, and add the estimated X-ray photons from their corresponding $\text{SFR}_{Ly\alpha}$ to analyse the probability on $f_{Ly\alpha}^{Esc}$. By coadding all LAEs between redshift $z = 2$ and 6.5 , the estimated counts are plotted in Figure 3 as a function of $f_{Ly\alpha}^{Esc}$. The signal should be $S/N > 3$ when $f_{Ly\alpha}^{Esc} < 5.7\%$, and $S/N > 1$ when $f_{Ly\alpha}^{Esc} < 17\%$. So we can reject the value of 5% at 99.87% confidence level, and report that the real value of $f_{Ly\alpha}^{Esc} > 17\%$ in 84% confidence level. Our lower limit is larger than the $f_{Ly\alpha}^{Esc} \simeq 0.1$ at $z=3$ from the cosmological SPH simulation of LAEs (Nagamine et al. 2010).

5.2. $f_{Ly\alpha}^{Esc}(\text{X-ray})$ vs. $f_{Ly\alpha}^{Esc}(\text{UV/Opt.})$

The escape fraction of LAEs have also been discussed by Atek et al. (2009) for $z = 0.3$ LAEs by using extinction-corrected $H\alpha$ to $Ly\alpha$ ratio, which has a ranges from $f_{Ly\alpha/H\alpha}^{Esc} \sim 10\%$ to 100% , and Blanc et al. 2010 for $1.9 < z < 3.8$ LAEs through extinction-corrected UV to $Ly\alpha$ ratio as average $f_{Ly\alpha/UV_corr}^{Esc} \sim 22\%$. The $f_{esc}^{Ly\alpha}$ for LAEs estimated from the ratio of $SFR_{Ly\alpha}$ and dust-corrected SFR_{UV} , $f_{Ly\alpha/UV_corr}^{Esc} = SFR_{Ly\alpha}/(SFR_{UV}/10^{-A_{1200}/2.5})$, also exist for our sample. Guaita et al. (2011), Gawiser et al. (2007) and Nilsson et al. (2007) did the stacked SED fitting on the samples at $z = 2.1 \sim 3.2$. At $z \sim 0.3$ and 4.5 , Finkelstein et al. (2008, 2010) did individual SED fitting for LAEs with existing *Hubble* and *Spitzer* observations. The dust properties of the SED fitting results at different redshifts are converted to A_{1200} (see in table 3) using Calzetti et al. (2000). The $f_{Ly\alpha/UV_corr}^{Esc}$ from dust-corrected UV to $Ly\alpha$ ratio for our sample show no evolution from $z \sim 2$ to $z \sim 3.2$, as $f_{Ly\alpha/UV_corr}^{Esc} \sim 26\%$, and is consistent with $\sim 22\%$ of Blanc et al. 2010. At $z \sim 4.5$, the SED fitting results might be affected by the poor spatial resolution of *Spitzer*. As an independent estimate on $f_{Ly\alpha}^{Esc}$ from X-ray, our $f_{Ly\alpha}^{Esc}$ at $z = 0.3$ are located at the low end of Atek et al. (2009), while consistent at $1.9 < z < 3.8$ with Blanc et al. 2010 (see figure 2), and the $f_{Ly\alpha/UV_corr}^{Esc}$ from the SED fitting results at $z = 2.1, 3.1, 3.2$ and 4.5 . The LAEs at $z \sim 0.3$ seems different compared to high-redshift LAEs, as they are more AGN contaminated (AGN fraction of $\sim 15\% - 40\%$, e.g., Scarlata et al. 2009; Cowie et al. 2010; Finkelstein et al. 2009a) and more massive and dusty. At high-redshift, the AGN fraction in LAEs is very low (AGN fraction $\lesssim 5\%$, Zheng et al. 2010 and references there in), and AGNs are relatively easy to detect in this deepest *Chandra* field, so the lower limit of $f_{esc}^{Ly\alpha}$ should be very robust. Our X-ray constraints on the $f_{Ly\alpha}^{Esc}$, as well as the $f_{Ly\alpha/UV_corr}^{Esc}$ estimated from SED fitting, show that the $Ly\alpha$ escape fraction might not evolve during the redshift $2.1 \leq z \leq 3.2$.

Hayes et al. (2011) and Blanc et al. (2010) also reported the global evolution of $f_{esc}^{Ly\alpha}$, which is defined as the ratio of integrated $Ly\alpha$ luminosity functions from LAEs and the global extinction-corrected SFR density at different redshift. The global extinction-corrected SFR densities were integrated from $H\alpha$ or UV luminosity. However, we should point out that at $z \sim 1, 3, 4$, and 5 , the SFR_X from LBGs are consistent with SFR_{UV} corrected with dust extinction (Nandra et al. 2002, Lehmer et al. 2005). This means that with the X-ray stacking on LBGs, we should get the same global SFR ($M_{\odot} yr^{-1} Mpc^{-3}$) as from integrating the UV luminosity.

5.3. Uncertainties in empirical $SFR_X - L_X$ Calibration

To constrain the accurate value of $f_{Ly\alpha}^{Esc}$ from X-ray, it is very important to determine the relationship between SFR_X and L_X . Unfortunately, all the calibrations use galaxies at $z \lesssim 1$. Nandra et al. 2002, Grimm et al. 2003, and Ranalli et al. 2003 derive a linear $L_X - SFR_X$ relationship. Colbert et al. (2004) and Lehmer et al. (2010) fit $L_X = \alpha \times M_* + \beta \times SFR_X$ to take into account

the contribution of LMXBs ($\alpha \times M_*$) together with HMXBs ($\beta \times SFR_X$)⁴. Their samples consist of local normal galaxies and luminous Infrared galaxies, respectively. These are too massive or too dusty compared to our LAE sample. Persic et al. (2004) resolved hard X-ray luminosity for HMXBs in nearby galaxies through their X-ray spectra, and assumed all the X-ray luminosity from $z \sim 1$ (the universe with an age of 6 Gyr) star-forming galaxies is due to HMXBs to derive a relationship³ of $L_{HMXBs} = \beta' \times SFR_X$. Tullmann et al. (2006) find a strong linear correlation between integrated soft X-ray (0.3–2.0 keV) and FIR for a sample of 23 edge-on late-type spiral galaxies, and their calibrated factor of SFR_X/L_{soft} is about 1.5~2 times larger than the factor of Ranalli et al.

We prefer to use the Ranalli et al. (2003) calibration of X-ray flux vs. SFR, because it is calibrated to local and $z \sim 1$ star-forming galaxies. Also, its application to high redshift LBGs show consistency between SFR_X and dust-corrected SFR_{UV} (Nandra et al. 2002, Lehmer et al. 2005). A recent study by Gorski et al. (in prep) on local blue compact dwarf galaxies, which are very metal poor (metallicities < 0.07 solar) and are like high redshift LAEs, show that their $SFR_{24\mu m}$ and $SFR_{H\alpha}$ equal to $1/10 \sim 1/5$ of SFR_X with Ranalli et al., which means that our lower limit on $f_{Ly\alpha}^{Esc}$ should be 5~10 times larger with the new relationship. We also find 6 X-ray detected LBGs (Zheng et al. in prep) from GALEX selected 420 $z \sim 1$ LBGs in CDF-S (Burgarella et al. 2007), their $SFR_{TIR} + SFR_{UV}$ equal to $\sim 1/2$ of SFR_X with Ranalli et al. X-ray stacking of the non-detected LBGs at $z \sim 1$ (Zheng et al. in prep) show $S/N \geq 3$ signal at rest-frame 0.5-2 keV band and 2-10 keV band with same average luminosity, which favors relationship of Ranalli et al., while no detected signal ($S/N < 1$) at rest-frame 10-16 keV band, at which energy band Persic et al. (2004) thought the X-ray flux were mainly from HMXBs for high- z star-forming galaxies.

Had we chosen a different calibration for the SFR_X we would infer 2~3 times (5 times with Persic et al.) larger SFR_X than with the relationship of Ranalli et al. (2003) for our $z > 2$ LAEs ($\alpha \times M_*$ should be negligible with Colbert et al. and Lehmer et al. relation). Therefore the systematic uncertainties on the derived SFR_X , and hence the escape fraction of Ly α photons is about a factor of 3. These uncertainties ($\sim 0.1-3$) for SFR- L_X relationship can be decreased with future *Chandra* deep observations on star-forming galaxies at low metallicities, or more LAEs/LBGs at redshift $\lesssim 2$ in CDFS, which are perhaps the closest analogs to high redshift Ly α galaxies.

5.4. Implications from simulated SFR_X - L_X relationship

We should note that the X-ray radiation from galaxies is predicted to be quite low for very young stellar populations. Galaxies younger than 40 Myr may not show enough soft x-rays (from

⁴Here X-ray range of 0.3–8 keV and 2–10 keV, $\alpha = (1.3 \pm 0.2)$ and $(0.905 \pm 0.037) \times 10^{29} \text{ erg s}^{-1} M_{\odot}^{-1}$, and $\beta = (0.7 \pm 0.2)$ and $(1.62 \pm 0.22) \times 10^{39} \text{ erg s}^{-1} (M_{\odot} \text{ yr}^{-1})^{-1}$ for Colbert et al. and Lehmer et al., separately. Note that $L_{0.3-8keV} \sim 2 \times L_{2-10keV}$ for $\Gamma = 2$ and no dust extinction. $\beta' = 10^{39} \text{ erg s}^{-1} (M_{\odot} \text{ yr}^{-1})^{-1}$ for $L_{2-10keV}$ Persic et al. 2004.

SNR and hot gas, Mas-Hesse et al. 2008) proportional to their intrinsic SFRs, and galaxies younger than 15 Myr may not have enough hard x-ray emission (from HMXBs, Mas-Hesse & Cervino 1999) proportional to their intrinsic SFRs. Mas-Hesse et al. (2008) predict the soft X-ray to far infrared luminosities ratio in star-forming galaxies from synthesis models. They find that the ratio is dependent on the age of the star formation episode, and expected to stabilize only after around 30 Myr. After 30 Myr, the correlation becomes stable and is consistent with $\text{SFR}_X - L_{soft}$ of Ranalli et al. 2003. In hard X-ray band, Mas-Hesse & Cervino (1999) predicted that a few HMXB should be active in starbursts that are older than 5-6 Myr, contributing a few times 10^{38} erg s^{-1} to the total X-ray luminosity. Recent *Chandra* studies in the Antennae (Rangelov et al. in prep) found 22 of 82 X-ray binaries coincident or nearly coincident with star clusters, and the ages of the clusters were estimated by comparing their multi-band colors with predictions from stellar evolutionary models. They found 14 of the 22 coincident sources are hosted by star clusters with ages of ~ 6 Myr or less. So the HMXBs in star-forming galaxies might form earlier than we thought from the simulations. The estimates on LAEs' age are based on SED fitting and are quite uncertain. The fitting results of LAEs' SED are reported at $z = 2.1$ (Guaita et al. 2011), 2.25 (Nilsson et al. 2009), 3.1 (Gawiser et al. 2007), 4.5 (Finkelstein et al. 2008) and $z=4.0-5.5$ (Pirzkal et al. 2007). All the results show that the best fit age parameter is 20~40 Myr, but extend to $\sim 0.1-1$ Gyr at the 68% confidence level. So if $\sim 25\% = (20 \text{ Myr} - 15 \text{ Myr}) / (40 \text{ Myr} - 20 \text{ Myr})$ of the LAEs are younger than 15 Myrs, the estimated SFR should be 1/3 times larger, and that will decrease our $f_{Ly\alpha}^{Esc}$ by a factor of 3/4.

Conclusions: From the 4 Ms X-ray *Chandra* image of CDF-S we coadded 69 $Ly\alpha$ emitting galaxies between redshifts $2 < z < 6.5$. None of these galaxies were individually detected. The absence of signal in the coadded image implies an average flux of less than 7.6×10^{-19} ergs cm^{-2} s^{-1} (1-sigma). This implies that the SFRs in these galaxies are quite modest, as indicated by the $Ly\alpha$ line emission. And the ratio of the average $Ly\alpha$ line intensity to the upper limits of X-ray flux constrain the $Ly\alpha$ escape fraction of $f_{Ly\alpha}^{Esc} > 17\%$ at 84% confidence level.

Acknowledgements: ZYZ would like to thank the support from the China Scholarship Council (CSC No. 2009634062) and Arizona State University. SM & JER are supported by the United States National Science Foundation grant AST-0808165. The work of JXW is supported by National Basic Research Program of China (973 program, Grant No. 2007CB815404), and Chinese National Science Foundation (Grant No. 10825312).

Table 1. GALEX and CHANDRA observation of two $z \sim 0.3$ LAEs in the central CDF-S region.

			Optical Information					
R.A. (deg)	Dec. (deg)	redshift	Mass ^a ($\times 10^9 M_\odot$)	EW (\AA)	$\log L_{Ly\alpha}$ (ergs s ⁻¹)	SFR _{Lyα} (M_\odot yr ⁻¹)		
53.2360	-27.8879	0.374	4.6 \pm 0.2	23.2	42.3	2.0		
53.2803	-27.7424	0.219	107.7 \pm 9.5	11.8	41.5	0.3		
			X-ray Information					
R.A. (deg)	Dec. (deg)	redshift	NH ($\times 10^{22}$ cm ⁻²)	$\log L_{0.5-2}$ (ergs s ⁻¹)	$\log L_{2-10}$ (ergs s ⁻¹)	SFR _{X,C}	SFR _{X,R-hard} (M_\odot yr ⁻¹)	SFR _{X,R-soft}
53.2360	-27.8879	0.374	3.2	40.8	41.6	567.9	79.6	13.9
53.2803	-27.7424	0.219	2.2	40.2	40.9	93.5	15.9	3.5

^aThe galaxy mass of the two LAEs are from their SED fitting of Finkelstein et al. 2009, and the values of EW and $L_{Ly\alpha}$ are from Deharveng et al. 2008.

^bThe SFR_{X,C}, SFR_{X,R-hard} and SFR_{X,R-soft} for the two $z \sim 0.3$ LAEs are calculated with Colbert et al. 2004, L_{hard} -SFR_X and L_{soft} -SFR_X relations of Ranalli et al. 2003, respectively.

Table 2. Stacking results of undetected LAEs located in the CDF-S and ECDF-S Field with off-axis-angle $< 6'$.

Redshift	Number ^a	Time Ms	X-ray COUNTS ^b						$F_X(> 1\sigma)^c$			$\lg_{10}(L_X(> 1\sigma))^c$ $L_{2-10keV}$	$SFR_X(> 1\sigma)^c$ ($M_{\odot} \text{ yr}^{-1}$)
			Tot _S	Net _S	Tot _H	Net _H	Tot ₀₅₋₇	Net ₀₅₋₇	F _{soft}	F _{hard}	F _{full}		
CDF-S only, 50 % PSF extraction													
2.1	12	39.1	20.	-4.3	71.	11.5	91.	7.1	0.19	2.54	0.98	40.8	14
3.1	18	59.2	50.	-4.9	120.	-8.2	170.	-13.0	0.18	0.96	0.51	41.2	32
3.2	23	73.9	54.	-9.4	145.	-3.5	199.	-12.9	0.15	0.84	0.44	41.1	28
4.5	12	39.3	30.	2.5	59.	-6.8	89.	-4.3	0.31	1.05	0.58	41.8	139
5.7	3	9.8	12.	-0.6	34.	5.9	46.	5.4	0.62	6.19	2.90	42.3	439
6.5	1	3.3	3.	-3.6	16.	0.6	19.	-2.9	1.17	8.16	3.53	42.7	1002
CDF-S + ECDF-S, 50 % PSF extraction													
0.3	2 ^d	0.4	2.	1.8	1.	0.6	3.	2.4	12.87	30.77	25.25	40.9	16
2.1	122	72.2	49.	1.9	125.	11.7	169.	9.1	0.18	1.54	0.68	40.8	14 ₁
3.1	118	85.8	71.	-6.2	169.	-3.4	234.	-12.4	0.14	0.76	0.40	41.1	28 ₃
3.2	24	74.9	55.	-9.1	159.	5.9	216.	-2.7	0.15	1.24	0.45	41.1	28 ₁
4.5	64	49.8	44.	6.8	93.	6.8	136.	13.7	0.38	1.65	1.13	41.9	160
5.7	17	12.6	14.	-0.0	37.	5.6	51.	5.6	0.50	4.73	2.33	42.3	440
6.5	6	4.5	4.	-3.0	19.	2.8	23.	-0.2	0.93	8.55	2.79	42.6	876

^aNumber of LAEs located in central CDF-S and ECDF-S region selected for stacking analysis. Reference: LAEs at $z \sim 0.3$ from Deharveng et al. (2008), $z = 2.1$ from Guaita et al. 2010, $z = 3.1$ from Gronwall et al. 2007 and Ciardullo et al. 2011, $z = 3.15$ from Nilsson et al. 2007, $z = 4.5$ from Finkelstein et al. 2009, $z = 5.7$ from Wang et al 2005 and $z = 6.5$ from Rhoads et al. ???.

^bNotice that the number of counts are extracted from their 50% PSFs and summed up, and not corrected for the apertures.

^cThe 1σ flux limits are obtained by first calculating the 1σ upper limit on counts as $Net+1 \times (\sqrt{Tot+0.75} + 1) / (\text{PSF-fraction})$. Here “Net” and “Tot” are the net and total counts in the 50% PSF region, respectively, while “PSF-fraction” here is 50%. The counts are then divided by effective integration time and multiplied by the count-rate to flux conversion factor. The tabulated flux limits are in units of

10^{-17} ergs cm $^{-2}$ s $^{-1}$. The SFR_X for all LAEs at $z>2$ are converted with the relationship of Ranalli et al. 2003 from $1-\sigma$ upper limit on $L_{2-10\text{keV}}$.

^dThe two $z\sim 0.3$ LAEs (the same sources in Table 1) only show upper limits in ECDF-S region, where their upper limits meet well with the detection in 4Ms CDF-S exposure.

Table 3. Our unitive LAE samples and their average SFRs and average Ly α escape fractions in the 4Ms CDF-S region.

Redshift	SFR $_X^b$	SFR $_{Ly\alpha}^b$ (M $_{\odot}$ yr $^{-1}$)	SFR $_{UV}^b$	A $_{1200}^c$ (mag)	f $_{(Ly\alpha/UV_corr)}^{esc\ d}$ (%)	f $_{(Ly\alpha/X)}^{esc\ e}$ (%)
0.219	3.5-16	0.3	2.9	1.25 \pm 0.35	3.3 $^{+1.2}_{-1.0}$	1.9-8.6
0.374	13.9-80	2	6.2	2.00 \pm 0.00	5.1	2.5-14.4
2.1	<14	1.9	2.4	1.2 $^{+0.5}_{-1.2}$	26 $^{+53}_{-9}$	>14
3.1	<28	2.6	5.3	< 0.6	28 $^{+21}_{-0}$	>9.4
3.2	< 28	2.3	4.2	0.8 $^{+0.3}_{-0.5}$	26 $^{+16}_{-6}$	>8.3
4.5	< 139	6.0	24	1.5 $^{+3}_{-1.1}$	6 $^{+11}_{-5.6}$	>4.3
5.7	< 439	5.5	>1.3
6.5	<876	5	>0.57

^aThe results of LAEs at $z \sim 0.3$ are individually detected, and the results of LAEs at $z > 2$ are stacked or averaged.

^bThe SFR $_X$ for all LAEs at $z > 2$ are converted with the relationship of Ranalli et al. 2003 from 1- σ upper limit on L $_{2-10keV}$. The SFR $_{Ly\alpha}$ and SFR $_{UV}$ are converted with Kennicutt 1998.

^cThe A $_{1200}$ were converted from the dust properties of different SED fitting papers under Calzetti et al. (2000) dust law: Finkelstein et al. 2010 for $z \sim 0.3$ LAEs, Guaita et al. 2011 for $z \sim 2.1$ LAEs, Gawiser et al. 2007 for $z \sim 3.1$ LAEs, Nilsson et al. 2007 for $z \sim 3.15$ LAEs, and Finkelstein et al. 2008 for $z \sim 4.5$ LAEs.

^dThe Ly α escape fraction estimated from extinction-corrected UV flux:

$$f_{(Ly\alpha/UV)}^{esc} = \frac{SFR_{Ly\alpha}}{SFR_{UV}/10^{-(A_{1200}/2.5)}}.$$

^eThe Ly α escape fraction estimated from X-ray SFR: $f_{(Ly\alpha/X)}^{esc} = \frac{SFR_{Ly\alpha}}{SFR_X}$.

REFERENCES

- Atek, H., Kunth, D., et al. 2009, *A&A*, 506, L1
- Blanc, G. A., Adams, J. et al. 2010, *astro-ph/1011.0430*
- Burgarella, D., et al. 2007, *MNRAS*, 380, 986
- Calzetti, D., et al. *ApJ*, 533, 682
- Colbert, E. J. M., Heckman, T. M., Ptak, A. F., et al. 2004, *ApJ*, 602, 231
- Cowie, L. L., & Hu, E. M. 1998, *AJ*, 115, 1319
- Cowie, L. L., Barger, A.J., & Hu, E. M. 2010, *ApJ*, 711, 928
- Dawson, S., Rhoads, J. E., Malhotra, S., et al. 2007, *ApJ*, 671, 1227
- Deharveng, J. M., Small, T., et al. 2008, *ApJ*, 680, 1072
- Dickey, J. & Lockman, F., 1990, *ARA&A*, 28, 215
- Finkelstein, S. L., Rhoads, J. E., Malhotra, S., Grogan, N., & Wang, J. X. 2008, *ApJ*, 678, 655
- Finkelstein, S. L., Cohen, S. H., Malhotra, S., Rhoads, J. E., et al. 2009a, *ApJ*, 703, 162
- Finkelstein, S. L., Cohen, S. H., Malhotra, S., & Rhoads, J. E. 2009b, *ApJ*, 700, 276
- Finkelstein, S. L., Rhoads, J. E., Malhotra, S., & Grogan, N. 2009c, *ApJ*, 691, 465
- Finkelstein, S. L., Cohen, S. H., Moustakas, J., et al., 2010, *astro-ph/1012.4010*
- Finkelstein, S. L., Hill, G. J., et al. 2011, *ApJ*, 729, 140
- Gawiser, E., Francke, H., Lai, K., et al., 2007, *ApJ*, 671, 278
- Gehrels, N. 1986, *ApJ*, 303, 336
- Gilfanov, m., Grimm, H. J., Sunyaev, R., 2004, *NuPhS*, 132, 369
- Grimm, H.J., Gilfanov, M., & Sunyaev, R., 2003, *MNRAS*, 339, 793
- Gronwall, C. et al. 2007, *ApJ*, 667, 79
- Guaita, L., Gawiser, E., et al. 2010, *ApJ*, 714, 255
- Guaita, L., Gawiser, E., et al. 2011, *astro-ph/1101.3017*
- Hansen, M. & Oh, S. P. 2006, *MNRAS*, 367, 979
- Hayes, M., Ostlin, G. , et al. 2010, *Nature*, 464, 562
- Hayes, M., Schaerer, D., et al. 2011, *ApJ*, 730, 8
- Hu, E. M., Cowie, L. L., et al. 2004, *AJ*, 127, 563
- Iye, M., Ota, K, Kashikawa, N., et al. 2006, *Nature*, 443, 14
- Kennicutt, R. C., Jr. 1998, *ARA&A*, 36, 189
- Laird, E.S., Nandra, K., et al. 2005, *MNRAS*, 359, 47

- Laird, E.S., Nandra, K., Hobbs, A., & Steidel, C.C. 2006, MNRAS, 373, 217
- Lehmer, B.D., Brandt, W. N., et al. 2005, ApJS, 161, 21
- Lehmer, B.D., Brandt, W. N., et al. 2008, ApJ, 681, 1163
- Lehmer, B.D., Alexander, D.M., et al. 2010, ApJ, 724, 559
- Luo, B., Bauer, F. E., Brandt, W. N., et al. 2008, ApJS, 179, 19
- Malhotra, S. & Rhoads, J.E. 2002, ApJL, 565, 71
- Malhotra, S., Wang, J, Rhoads, J. E., et al. 2003, ApJ, 585, L25
- Martin, C. L., et al. 2008, ApJ, 679, 942
- Mas-Hesse, J. M. & Cervino, M. 1999, IAUS, 193, 550
- Mas-Hesse, J. M., Oti-Floranes, H., & Cervino, M. 2008, A&A, 483, 71
- Nagamine, K., Ouchi, M., Springel, V., Hernquist, L. 2010, PASJ, 62, 1455
- Nandra, K., Mushotzky, R. F., Arnaud, K., et al. 2002, ApJ, 576, 625
- Nilsson, K. K., Moller, P., Moller, O., et al. 2007, A&A, 471, 71
- Nilsson, K. K., Tapken, C., et al. 2009, A&A, 498, 13
- Neufeld, D. A. 1991, ApJL, 370, 85
- Partridge, R. B. & Peebles, P. J. E. 1967, ApJ, 148, 377
- Persic, M., Rephaeli, Y. et al. 2004, A&A, 419, 849
- Pirzkal, N., et al. 2004, ApJS, 154, 501
- Pirzkal, N., Malhotra, S., Rhoads, J. E., Xu, C. 2007, ApJ, 667, 49
- Ranalli, P., Comastri, A., & Setti, G. 2003, A&A, 399, 39
- Rhoads, J. E., Malhotra, S., et al. 2000, ApJL, 545, 85
- Rhoads, J. E., dey, A., Malhotra, S., et al. 2003, AJ, 125, 1006
- Rhoads, J. E., 2009, ApJ, 697, 942
- Scarlata, C. et al. 2009, ApJL, 704, 98
- Tullmann, R., et al. 2006, A&A, 457, 779
- Venemans, B. P., et al. 2005, A&A, 431, 793
- Wang, J. X., Rhoads, J. E., Malhotra, S., et al. 2004, ApJL, 608, 21
- Wang, J. X., Zheng, Z. Y., Malhotra, S., et al. 2007, ApJ, 669, 765
- Wang, J. X., Malhotra, S., Rhoads, J. E., et al. 2009, ApJ, 706, 762
- Zheng, Z. Y., Wang, J. X., Finkelstein, S. L., Malhotra, S., Rhoads, J. E., & Finkelstein, K. D. 2010, ApJ, 718, 52

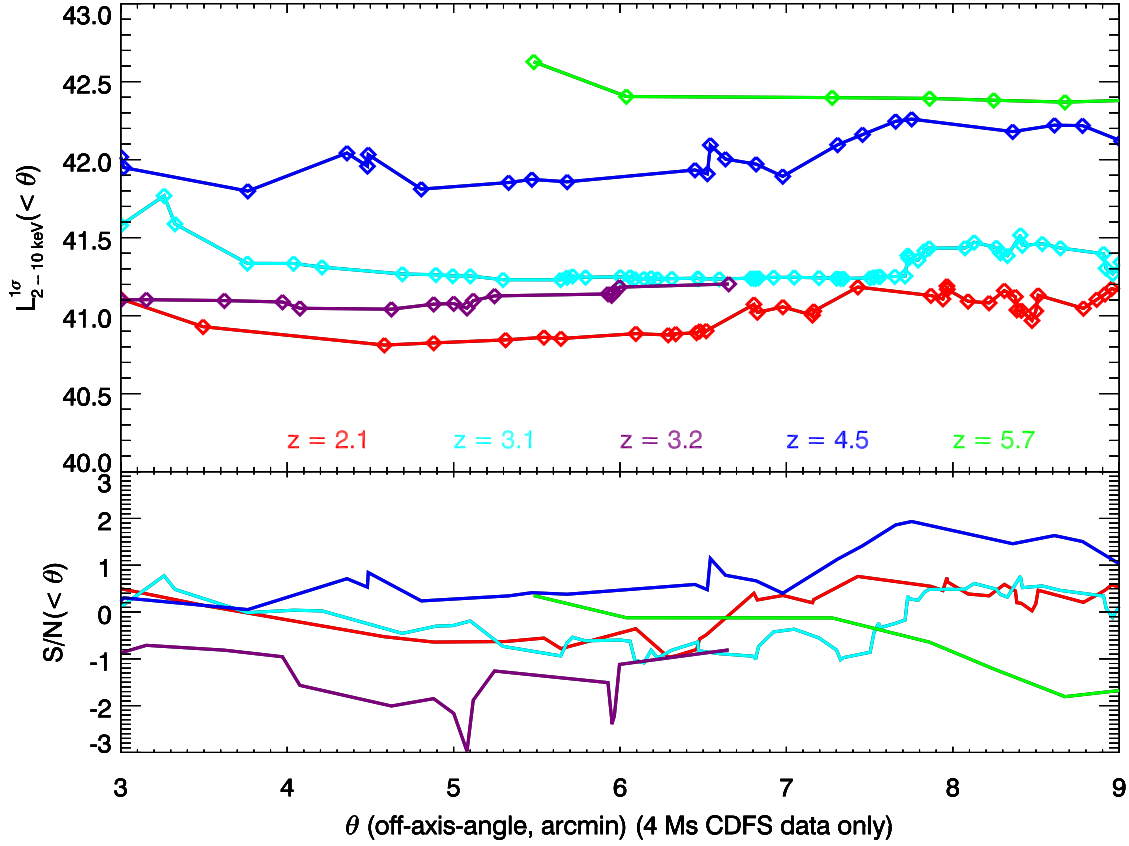


Fig. 1.— The X-ray stacking results for LAEs located within off-axis-angle $< \theta$ in the 4 Ms CDF-S data. The lower plot shows the signal-to-noise ratio of the stacked signal, and the upper plot shows the $1\text{-}\sigma$ upper limit on $L_{2-10\text{keV}}$ from the stacked signal. It can be seen that the upper limits on $L_{2-10\text{keV}}$ tend to increase when stacking LAEs located with $\theta \gtrsim 6.5$ arcmin. In this work the upper limit on f_X and L_X are extracted from stacking LAEs located within an off-axis angle $\theta < 6$ arcmin.

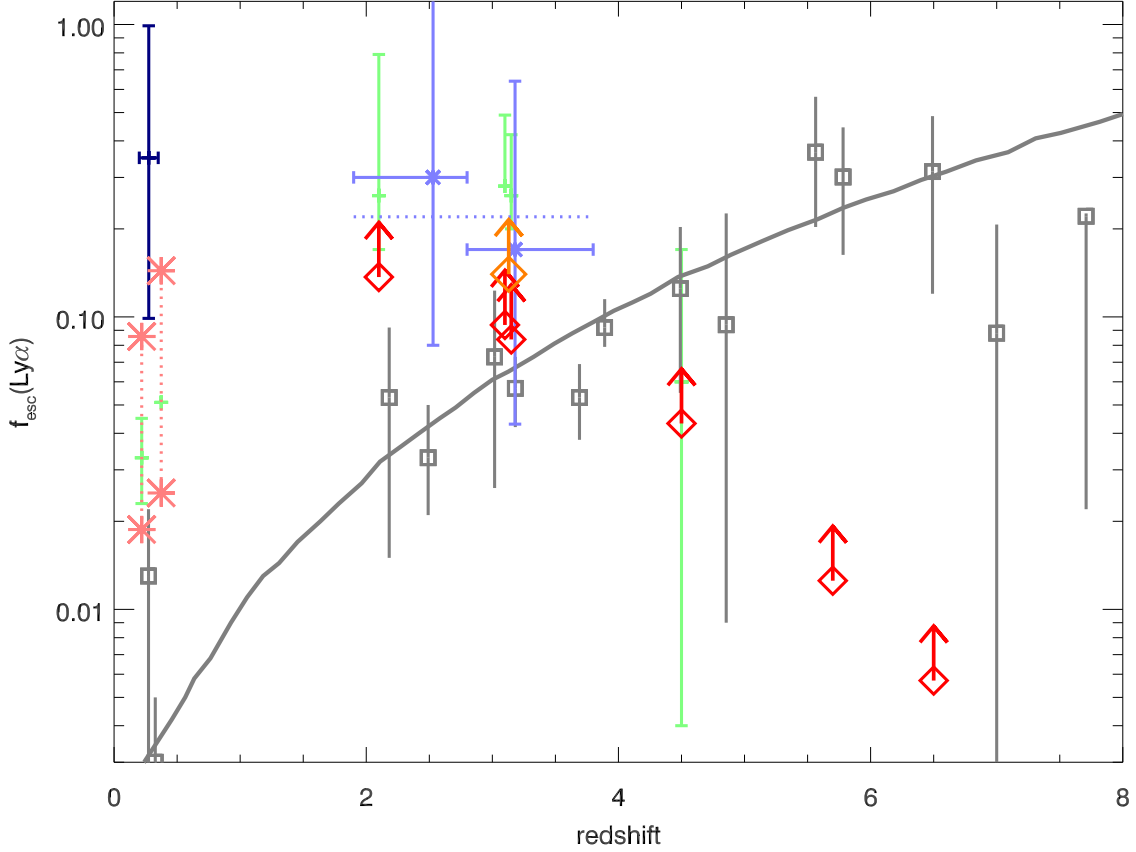


Fig. 2.— Ly α escape fraction estimated from Optical (navy cross: $f_{Ly\alpha}^{Esc}$ of $z \sim 0.3$ LAEs from Atek et al. 2009; light blue crosses and dotted lines: $f_{Ly\alpha}^{Esc}$ from blank field spectroscopic survey of 98 LAEs at $1.9 < z < 3.8$ from Blanc et al. 2010; green crosses: $f_{Ly\alpha}^{Esc}$ from SED fitting results of our sample, grey squares: global $f_{Ly\alpha}^{Esc}$ extracted from figure 1 of Hayes et al. 2011) compared with estimated from X-rays (light red: two LAEs with X-ray detections at $z \sim 0.3$; red: $f_{Ly\alpha}^{Esc}$ lower limits for LAEs at $z = [2.1, 3.1, 3.2, 4.5, 5.7, 6.5]$). Note that at $z > 4$, there are not enough data to constrain on X-ray derived $f_{Ly\alpha}^{Esc}$. The orange diamond are the combined upper limit at $z \sim 3$. The grey line is the best-fit constraint on the redshift evolution of global $f_{esc}^{Ly\alpha}$ derived by Hayes et al. 2011.

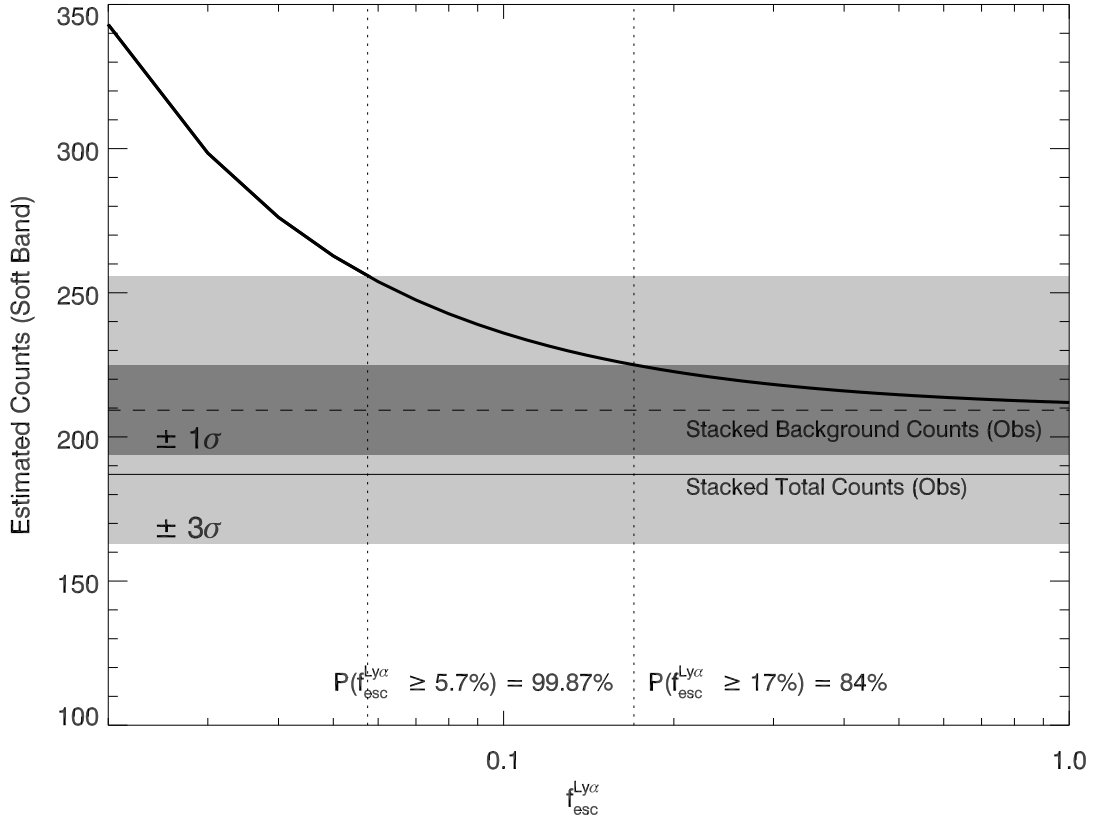


Fig. 3.— The estimated X-ray total counts as a function of $f_{esc}^{Ly\alpha}$ for all LAE candidates in CDF-S at $2 < z < 7$. Note that the observed total count (the solid horizontal line) in soft X-ray band is lower than the background count (the dashed horizontal line). The two dotted vertical lines imply where the estimated signal reach 1- σ and 3- σ level.